# Midband solitons in nonlinear photonic crystal resonators

Kęstutis Staliūnas*
*Institució Catalana de Recerca i Estudis Avançats (ICREA), Departament de Fisica i Enginyeria Nuclear, Universitat Politecnica de Catalunya (UPC), Colom 11, E-08222 Terrassa, Barcelona, Spain*
(Received 1 March 2004; published 2 July 2004)

We investigate cavity solitons in nonlinear photonic crystal resonators, i.e., in the nonlinear resonators with the refractive index periodically modulated in the transverse direction. We study several families of the cavity solitons: (1) "normal," and (2) "staggered" solitons, similar to those in conservative nonlinear photonic crystals; (3) "midband" solitons, predicted recently in dissipative nonlinear photonic crystals [K. Staliunas, Phys. Rev. Lett. **91**, 053901 (2003)]; and (4) "double head" cavity solitons not reported before. We investigate the solitons by (1) numerically solving the full microscopic model explicitly accounting for the small scale refractive index modulation, and (2) adopting a "mean field" approximation, e.g., eliminating the small scale refractive index modulation.

DOI: 10.1103/PhysRevE.70.016602 PACS number(s): 42.65.Tg, 05.45.Yv, 05.65.+b, 89.75.−k

## I. INTRODUCTION

Cavity solitons (CS), sometimes also named dissipative spatial solitons, have been theoretically predicted for general case of bistable nonlinear optical resonators [1], and for different particular bistable nonlinear optical systems: lasers with saturable absorber [2], two-photon lasers [3], optical parametric oscillators [4], semiconductor microresonators [5]. In several systems the CSs have been so far demonstrated experimentally: in lasers with saturable absorbers [6], in four wave mixing [7], and in semiconductor microresonators [8]. The interest on CS is in particular stimulated by their potential application for parallel information processing and storage [9]. The CS being bistable can be switched on and off, therefore they can serve as elementary memory element (can store one bit of information). The CSs can be excited in arbitrary place in the transverse plane of the resonator, which gives additional possibilities of their manipulation and application.

The most of the previous studies of CSs [1–9] assume that the nonlinear resonators are homogeneous in lateral direction. In fact the lateral boundary conditions are sometimes considered, e.g., accounting for the finite width of the aperture of the optical system. Here, under lateral homogeneity, we mean that the bulk area of the system is homogeneous on the spatial scale of the width of soliton, or less. Recent technologies allow manufacturing nonlinear resonators with some parameters (refraction index, nonlinearity, losses) laterally modulated on the spatial scale of a micron and less, i.e., on the scale much less than the typical spatial size of solitons. The typical size of the experimentally observed solitons is several tenths of microns: in the ever realized smallest soliton supporting systems, the semiconductor microresonators, with full cavity length $L \approx 5$ $\mu$m, the width of the soliton is $x_0 \approx 15$ $\mu$m as observed in [8]. The rapidly advancing micro- and nanotechnologies give a motivation for our study of cavity solitons in nonlinear resonators with spatially modulated refraction index on micron and submicron scale, i.e., in nonlinear photonic crystal resonators.

Another motivation follows from the results of the recent studies of spatial solitons in nonlinear ***nonresonator*** photonic crystals [10], where the nonlinear ***spatial*** propagation of the fields in the media with spatially modulated refraction index is studied. Recently the discrete Kerr-type solitons in propagation in materials with $\chi^{(3)}$ nonlinearity [11], as well as discrete parametric solitons in propagation in materials with $\chi^{(2)}$ nonlinearity [12] have been shown. These studies reveal a variety of families of discrete solitons. The basic ones are: (1) "normal" solitons with the carrier spatial wave number being around zero. They are the analogs of the spatial solitons in homogeneous nonlinear media; (2) "band-edge," or "staggered" solitons, with the carrier spatial wave number being around half of the modulation wave number. The field phase changes its value by $\pi$ between the modulation fringes across the staggered soliton, and the effective diffraction is of negative sign. In addition to these basic "normal" and "staggered" solitons, several intermediate discrete soliton states were reported ("zoology" of discrete solitons [13]). These results allow to expect that also the cavity solitons in nonlinear photonic crystal resonators can display a variety of shapes. Indeed several kinds of cavity solitons have been recently predicted in photonic crystal resonators [14]: These are "normal" and "staggered" cavity solitons, similar to those in conservative nonlinear photonic crystals, as described above. These are also narrow "midband" solitons, with the carrier spatial frequency between those for the "normal" and for the "staggered" solitons. The physical rationale behind the midband solitons is that if the effective diffraction is of positive sign for normal solitons, and of negative sign for band-edge ones, then there should be a point where the effective diffraction is zero, if the diffraction dependence curve is continuous. The spatial spectra of the "midband" soliton are centered around that zero-diffraction point, i.e., located close to the middle of the band of extended waves (hence the term midband solitons). Since the effective diffraction vanishes for the midband CSs, their size is no more limited by diffraction, but can be drastically reduced, comparing with the width of the "normal" solitons,

*Email address: kestutis.staliunas@icrea.es

 

i.e., literally to one wavelength [14]. The latter result gives a strong motivation to our studies, since the reduction of the size of the soliton is very desirable for technological applications.

In the present article we give a detailed numerical study of the above described families of the cavity solitons in nonlinear photonic crystal resonators. We also report a new family of the cavity solitons—the "double head" one.

Part of the results is obtained by a direct numerical integration of the equations for a laser with a saturable absorber for the laterally modulated refraction index. This (microscopic) model explicitly accounts for the small scale refractive index modulation. We chose this particular system of a laser with saturable absorber, because mathematically it is perhaps the simplest system, and physically is the most paradigmatic model for the optical bistability and for the CSs [2]. These results, however, can be generalized to other systems supporting cavity solitons.

Additionally we use a kind of "mean field" approach for the study of soliton properties, i.e., we reduce the full microscopic (small spatial scale) model by the equation accounting for the large scale spatial variation of the fields. The modulation of the refraction index is then accounted by respectively modified diffraction of the system. This results in a substantial reduction of the complexity, allows more precise studies of the asymptotic shapes of the CSs, also leads to analytical expressions of the soliton parameters (in particular of the width) depending on the parameters of the system.

## II. MODEL

The class A lasers with fast saturable absorber in paraxial- and mean field approximations is described by:

$$\frac{\partial A(\vec{r},t)}{\partial t} = \left( \frac{D_0}{1+|A|^2} - 1 - \frac{\alpha_0}{1+|A|^2/I_\alpha} + id\nabla^2 + g\nabla^2 + iV(\vec{r}) \right) \times A(\vec{r},t). \quad (1)$$

The right-hand side contains the terms of saturating gain, linear losses, saturating losses, diffraction, diffusion, and spatially varying refractive index: $V(\vec{r})=m(e^{iqx}+e^{-iqx})$, respectively. $D_0$ is the unsaturated gain, $\alpha_0$ is the unsaturated absorption, $I_\alpha$ is the saturation intensity of the absorber, $d=L\lambda Q/(4\pi)$ is the diffraction coefficient ($\lambda$ is the wavelength of the radiation, $L$ and $Q$ are the full length and finesse of the resonator), $g$ is the diffusion coefficient (usually $g \ll d$), and $m$ and $q$ are the amplitude and the wave number of the refractive index modulation in the transverse direction of resonator. See, e.g., also [2] for detailed description of the model (1).

The diffusion term lumps together the material diffusion (e.g., diffusion of population inversion), the limited width of the gain line, as well as the spatial frequency filtering. In most systems diffusion can be considered small compared with the diffraction (e.g., if the resonator mode is narrow compared with the atomic gain line). In our numerical study the diffusion/diffraction ratio is fixed to $g/d=10^{-4}$, but the results depend only negligibly on this ratio.

The field is considered to be dependent on one transverse dimension, and evolving in time. The field variation along the longitudinal direction was neglected. This mean field approximation is legitimate to the short and high-finesse resonators, like used to generate spatial solitons, e.g., in [8]. The numerical integration was performed using a split-step technique: by changing from the transverse space domain to the spatial Fourier domain in every integration step, which imposes periodic boundary conditions in transverse space of the resonator.

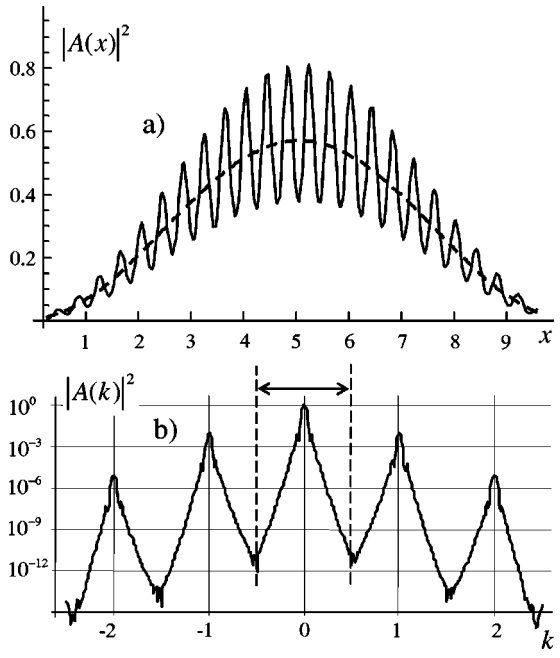


FIG. 1. The envelope (a) and the spatial power spectra (b) for the normal cavity solitons, as obtained by numerical integration of (1). Dashed lines represent the envelopes of the homogeneous field component of the soliton, obtained by filtering out spatial spectral components (retaining the spectral components as indicated by arrow in (b)). The parameters are: $I_\alpha=0.01$, $\alpha_0=5$, $D_0=1.7$, $d=1$, $q=15.89$, $m=25$ [$f=2m/(dq^2)=0.198$].

## III. NUMERICAL STUDY OF THE FULL MODEL

Figures 1–4 show the typical spatial profiles (a) and spatial power spectra (b) of stable cavity solitons, as obtained by numerical integration of (1).

(1) Normal soliton. This is the only possible family of solitons in the absence of spatial modulation of refraction index. When the refractive index is spatially modulated (with the spatial wave-number $q$), the modulation fringes of the soliton envelope appear [Fig. 1(a)] with the depth proportional to the amplitude of the refraction index modulation $m$. In a limit of weak modulation $m/(dq^2) \ll 1$ the modulation can be considered perturbatively. The spatial power spectrum [Fig. 1(b)] consists of a strong central component (at spatial carrier frequency), and of progressively decreasing sidebands. The effective diffraction of the radiation field is of positive sign, and is only weakly (perturbatively) effected by the lateral modulation of refraction index.

The dashed line in Fig. 1(a) shows the envelope of the soliton on a large spatial scale. The large scale soliton enve-

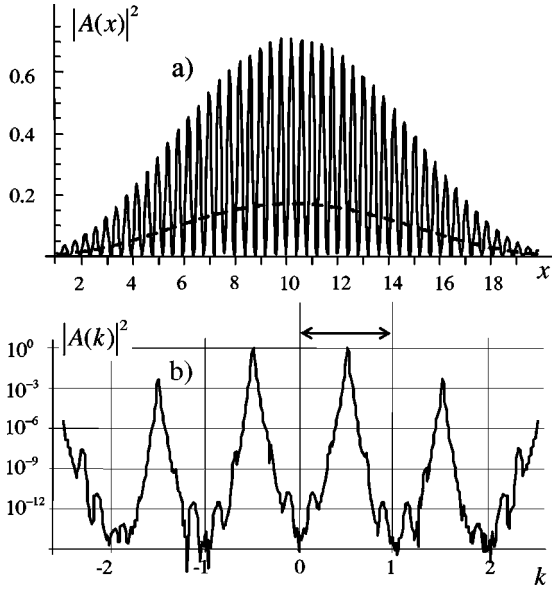


FIG. 2. The envelope (a) and the spatial power spectra (b) of a staggered soliton. Everything, except for the initial conditions, is as in Fig. 1.

lope was obtained by filtering out the sidebands from the spatial spectrum, and, using inverse Fourier transform, recovering the soliton constituents attributed to dominating spatial frequency [retaining the band of spatial frequencies as indicated by arrow in Fig. 1(b)].

(2) Staggered soliton (Fig. 2). The field phase changes by $\pi$ between the neighboring modulation fringes, therefore the field amplitude is modulated by 100%. The spatial power spectrum contains two strong components with the spatial frequencies at $k_0 \approx \pm q/2$. The staggered soliton is wider than

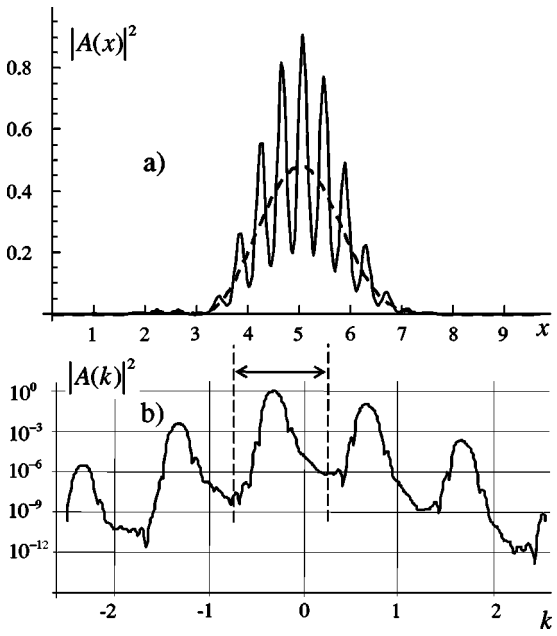


FIG. 3. The envelope (a) and the spatial power spectra (b) of the midband soliton. Everything, except for the initial conditions, is as in Fig. 1.

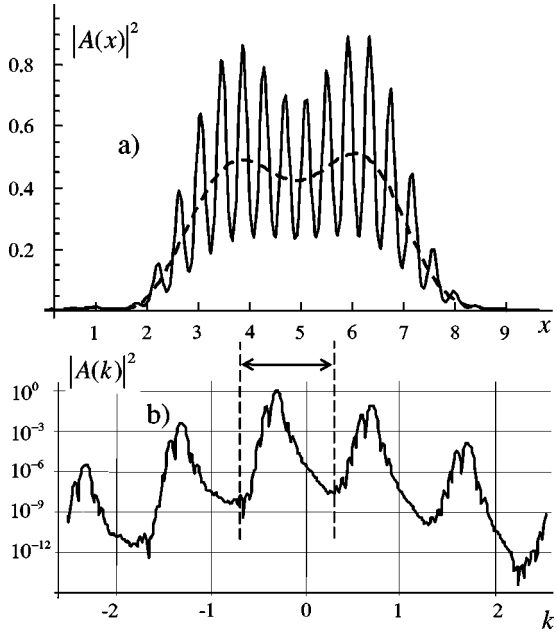


FIG. 4. The envelope (a) and the spatial power spectra (b) of the double head soliton. Everything, except for the initial conditions, is as in Fig. 1.

the normal one for the used parameter set (note the different spatial scales in Fig. 1 and Fig. 2). The staggered soliton has no analog in laterally homogeneous systems (the small scale spatial modulation by 100% cannot be considered as a small perturbation of soliton shape), and the effective diffraction of the soliton, as shown below, is of a negative sign.

(3) Midband soliton (Fig. 3). The spatial power spectrum contains a strong component centered at a spatial frequency $0 < k_0 < q/2$, i.e., at the wave number corresponding to zero diffraction. (Recall that the effective diffraction for normal soliton is positive, and for staggered soliton is negative, then there should exist a wave number with zero diffraction in between, if the dispersion curve is continuous.) The soliton is in general narrower in space than the normal and the staggered ones. Differently from the normal and the staggered solitons the midband soliton is never stationary, but moves with a constant velocity.

(4) Double-head soliton (Fig. 4). The spatial power spectrum of the double-head soliton is also double peaked, consisting of a dominating peak in the positive diffraction range, and the weaker peak in the negative diffraction range. One can consider such double-head solitons as the nonlinear superposition of a pair of two coupled solitons of positive and negative diffraction; however two heads of the soliton do not attribute to the two peaks in the domain of spatial frequencies, and are rather a result of interference of these two spatial frequencies. The double head soliton, like the midband one is never at rest, but runs with a constant velocity, dependent on the parameters.

The inverted double-head soliton was also observed, similar to the double-head soliton shown in Fig. 4. The difference is that the dominating peak appears in the negative diffraction range, and the weaker peak, in the positive diffraction range. In other words, the center of mass of the inverted

double-head soliton is located in the negative diffraction range (but also very close to zero diffraction point), in contrast to the double-head soliton shown in Fig. 4.

### IV. DISPERSION RELATION

In order to interpret the above numerical results, also in order to evaluate analytically the parameters of the solitons, the harmonic decomposition of the field components was performed, by considering dominating (two, or three) spatial harmonics of the field:

$$A(x,t) = e^{ik_0 x}[A_0(t) + A_1(t)e^{-iqx} + A_2(t)e^{+iqx}]. \tag{2}$$

Here the field components with the wave vectors $k_0$, $k_1 = k_0 - q$, and $k_2 = k_0 + q$ are considered. The linear evolution of waves in the resonator [Eq. (1) keeping only the linear in field amplitude and conservative terms] results in a linear system of coupled equations for the field components:

$$\partial A_0/\partial t = -idk_0^2 A_0 + imA_1 + imA_2, \tag{3a}$$

$$\partial A_{1,2}/\partial t = -idk_{1,2}^2 A_{1,2} + imA_0. \tag{3b}$$

The solution $\partial A_i/\partial t = i\omega A_i$, $i = 0,1,2$ of (3) exists, however does not lead to analytically tractable result. Figure 5(a) shows the solution of (3). The dashed lines show the dispersion relations for three uncoupled harmonic components of the field in absence of zero spatial modulation of the fields. For nonzero coupling the band gap appears and increases with increasing coupling of wave components. The parameters of the system (3) can be rescaled, and the number of relevant parameters reduced until two. Those are $f = 2m/(dq^2)$, a depth of a modulation induced by the spatially periodic perturbation, i.e., of a contrast of modulation fringes; and $k = k_0/q$, the carrier spatial wave number normalized to the spatial wave number of the modulation. Figure 5 is plotted using these normalized parameters.

Figure 5(b) shows the effective diffraction coefficient for the system of coupled waves calculated as $d_{\text{eff}} = -1/2\partial^2\omega/\partial k_0^2$ from the dispersion relation given by (3). The diffraction, as expected, changed its sign from plus to minus at some spatial frequency.

For the analytical treatment we considered either only two interacting field components (for the staggered, and midband solitons, where two components are dominant), or performed an asymptotical analysis of the solution of (3) (for the normal soliton, where all three components are relevant).

In two component case, neglecting $A_2$ ($A_2 \to 0$) the solution of (3) reads

$$\omega = \frac{dq^2}{2}[2|k| - 2k^2 - 1 \pm \sqrt{f^2 + (1-2|k|)^2}]. \tag{4a}$$

The effective diffraction $d_{\text{eff}} = -1/2\partial^2\omega/\partial k_0^2$ is:

$$d_{\text{eff}} = d\{1 - f^2/[f^2 + (1-2|k|)^2]^{3/2}\}. \tag{4b}$$

The diffraction becomes zero at a wave number: $k = (1 - \sqrt{f^{4/3} - f^2})/2$, according to (4b).

The asymptotical value of diffraction for the staggered CSs ($|k| = 1/2$) is $d_{\text{eff}} = d(1 - f^{-1})$, as follows from (4b), and is negative for small values of $f$. The width of the staggered soliton scales as $x_0 \propto \sqrt{|d_{\text{eff}}|} = \sqrt{d/f}$.

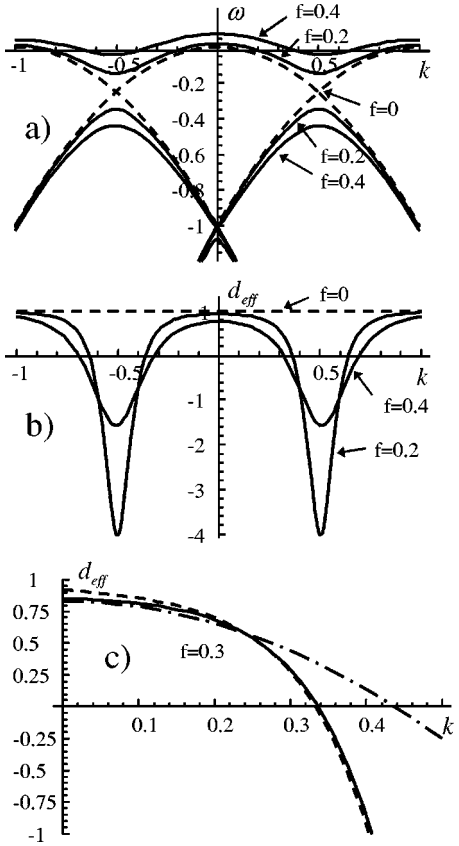


FIG. 5. Frequency (a) and diffraction (b) of linearly coupled plane waves, depending on the normalized spatial carrier frequency $k = k_0/q$, as given by the analytical solution of (3). The curves are plotted for different normalized coupling coefficients $f = 2m/(dq^2)$: $f = 0$ dashed, and $f = 0.2$, $f = 0.4$, solid. In (c) the diffraction coefficients followed from (3) (solid line), from (4b) (dashes line), and from (5b) (dashed-pointed line) are shown for $f = 0.3$.

The dependence of the diffraction coefficient as followed from (4b) is plotted by a dashed line in Fig. 5(c), and compared with the diffraction coefficient as followed from (3). The correspondence is good for large spatial frequencies (corresponding in particular to mid-band and staggered solitons), but gets worse for $k \to 0$ (corresponding to the normal CSs). This is because the dispersion relation (4a) and (4b) being valid when two field components dominate the dynamics (which is the case for staggered and midband solitons) is no more valid for normal solitons, with the carrier spatial wave number centered around $k = 0$. For normal solitons three field components are relevant, i.e., the strong homogeneous component, and two sidebands of nearly equal relevance. To evaluate the parameters of soliton in this limit we used the series expansion (with respect to $k$ and $f$) of the solution of (3) which for the upper solution branch results in

$$\omega = dq^2[f^2/2 + k^2(-1 + 2f^2) + 8f^2k^4], \tag{5a}$$

$$d_{\text{eff}} = d(1 - 2f^2 - 48k^2f^2). \tag{5b}$$

(5) indicates the decrease of the diffraction coefficient, and correspondingly of the size of the normal soliton $x_0 \propto \sqrt{|d_{\text{eff}}|}$

with the increasing amplitude of spatial modulation of refraction index. The diffraction coefficient (5b) is plotted in Fig. 5(c) by the dashed-pointed line, showing a good correspondence for $k \to 0$ with the diffraction coefficient following from the full treatment of (3).

## V. REDUCED EQUATIONS

The complexity of the full system (1) can be substantially reduced by eliminating the small spatial scales, related with the spatial modulation. A possibility for this reduction is hinted by the above linear analysis. Similarly as one decomposes the linearly evolving field into coupled components, one can decompose the nonlinearly interacting field into spatially dependent coupled field components:

$$A(x,X,t) = e^{ik_0 x}[A_0(X,t) + A_1(X,t)e^{-iqx} + A_2(X,t)e^{+iqx}]. \tag{6}$$

Here the microscopic field $A(x,X,t)$ depends on the small spatial scale $x$ (of the order of the spatial period of the modulation of refraction index), as well as on large spatial scale $X$ (of the order of soliton size). The coupled field components $A_i(X,t)$ $(i=0,1,2)$ depend on the large spatial scale only. Then, inserting (6) into (1), and considering that the spatial scales are well separated $x \ll X$ (which, written differently, means $|\nabla| \ll |q|$), one can derive a coupled set of equations for coupled field components:

$$\frac{\partial A_0}{\partial t} = N_0(A_0,A_{1,2}) + id(\nabla + ik_0)^2 A_0 + imA_1 + imA_2, \tag{7a}$$

$$\frac{\partial A_{1,2}}{\partial t} = N_{1,2}(A_0,A_{1,2}) + id(\nabla + ik_{1,2})^2 A_{1,2} + imA_0. \tag{7b}$$

Here the nonlinear operators $N_i(A_0,A_{1,2})$ are the projections of the nonlinearity into wave vectors centered around $k_i$, respectively $(i=0,1,2)$. We assume here for simplicity $g=0$. (7) is already a significant simplification of the problem, since it considers the variation of the fields on a large spatial scale only.

Further reduction of (7) is possible for $m \ll dq^2$ [equivalently for $f=2m/(dq^2) \ll 1$]. This results in the hierarchy of the field components $|A_{1,2}| \ll |A_0|$. Then, one can eliminate adiabatically the weak side-band fields $A_{1,2}$ assuming that they are enslaved by the dominating central component $A_0$, and thus systematically derive a single equation for the order parameter of the system (which is the field proportional to the homogeneous field component $A_0$) (see Appendix). However, instead of the systematical derivation, we write down phenomenologically the order parameter equation. One can easily construct the linear part of the order parameter equation from the dispersion relation (4) and (5). For definiteness we chose (4), which is more appropriate for the study of midband soliton, which results in:

$$\hat{L} = id\left(\nabla^2 - \frac{q^2}{2} + \frac{\sqrt{f^2q^4 + (q^2 + 2iq|\nabla|)^2}}{2}\right) + dq|\nabla|. \tag{8}$$

The coefficient $ik$ in spatial Fourier domain is here simply substituted by the differential operator $\nabla = \partial/\partial x$ in space domain. Analogously the coefficient $i\omega$ in temporal Fourier frequency domain is substituted by the time evolution operator $\partial/\partial t$ in the time domain. We complete the linear part [given solely by the operator $\hat{L}$ (8)] by nonlinear terms, which finally results in the order parameter equation:

$$\frac{\partial A_0(\vec{r},t)}{\partial t} = \left(\frac{D_0}{1+|A_0|^2} - 1 - \frac{\alpha_0}{1+|A_0|^2/I_\alpha} + \hat{L} + g\nabla^2\right)A_0(\vec{r},t). \tag{9}$$

The linear stability analysis of (9) reproduces, per definition, the dispersion curve (4). In the absence of spatial modulation, the (9) obviously converges into (1). Finally the above described adiabatic elimination, using the smallness assumptions: $A_0 = O(1)$, $m = O(\varepsilon)$, $dq^2 = O(1/\varepsilon)$, derives (9) systematically, by retaining the terms of smallness expansion up to the order $O(\varepsilon^3)$ (see Appendix). Due to the above smallness assumption the nonlinear term in the reduced Eq. (9) is identical to that in starting Eq. (1).

## VI. NUMERICAL STUDY: FULL EQUATIONS AND REDUCED MODELS

The derived order parameter Eq. (9) was checked by comparison of the numerical results from it and from full equation system (1). Figure 6 gives the shapes (the amplitude and phase profiles) of the midband CSs, indicating a good correspondence between the results obtained by models (1) and (9). In particular the results indicate a peculiarity of the midband CS: The shapes of the CS always show the main peak, and the small peak at the trailing edge of the CS. (We note that the amplitude profiles of fields are plotted in Fig. 6, in contrast to intensity profiles in Figs. 1–4, which enhances the visibility of the satellite peak.) The satellite peak is in antiphase to the dominating peak, as the phase profile indicates. The presence of the small satellite in antiphase to the main soliton is a good indication that the normal diffraction (second order spatial derivative) is absent and the diffraction of the next (third) order is dominating. The soliton shape resembles the temporal pulse shape after linear propagation in a fiber with dominating third order dispersion [15], or spatial pulse shape after linear propagation in the material with dominating third order diffraction [16].

In Fig. 7 the soliton size dependencies on the amplitude of spatial modulation are depicted. Several families are plotted corresponding to different values of the pump parameter $D_0$ within the stability range of the CS. Again a good correspondence between the results of integration of the full Eq. (1) (solid circles) and the reduced Eq. (9) open circles is obtained. The analytical evaluations (dashed curves) [(4b) and (5b)] are also in a good correspondence with the numerical results.

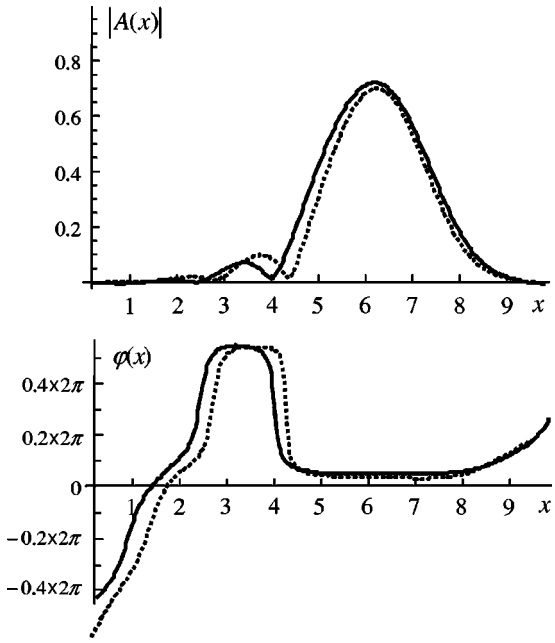


FIG. 6. Amplitude and phase profile of midband solitons, as obtained by numerical integration of (1) with subsequent filtering of spatial spectra, the solid line; and as obtained by numerical integration of mean field model (9) with the dispersion relation (4a), the dashed line. The parameters for numerical integration, as in Fig. 1. The soliton is propagating to the right (so the satellite is on a trailing edge of the soliton).

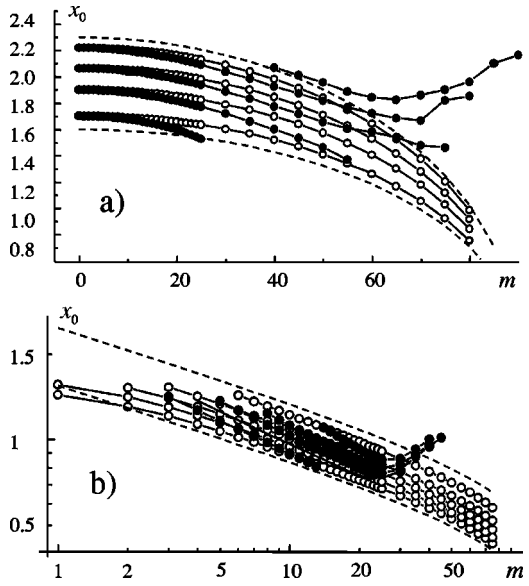


FIG. 7. The half-width of the normal (a) and the midband (b) CS, as calculated from numerical integration of the microscopic model (1) (the solid circles) and of the mean field model (9) (open circles), depending on the modulation amplitudes. The calculations were performed for different values of pump parameters for $D_0 = 1.59, 1.62, 1.65, 1.68, 1.71$ in case (a), and for $D_0 = 1.65, 1.68, 1.71, 1.74, 1.77$ in case (b) (spaced equidistantly within the stability range of the soliton). The dashed lines are the analytically evaluated width of the soliton as following from (5b) in case (a), and 4(b) in case (b). The parameters for numerical integration are as in Fig. 1.

## VII. CONCLUSIONS

Concluding, we show that the different families of the CSs exist in dissipative nonlinear resonators with the refractive index modulated in transversal plane, i.e. in nonlinear photonic crystal resonators. The variety of the families is due to spatial modulation of the refraction index, whereas only the normal solitons are possible for transversally homogeneous resonators.

We derive the order parameter equation, i.e., the equation depending on the fields of large spatial scale only. This allows a more precise study of the asymptotic shapes of the CSs, which also leads to analytical expressions of the soliton parameters. In particular the widths of the solitons belonging to different families were analytically estimated, based on the order parameter equation.

Among the reported families of solitons we pay largest attention to the narrow midband solitons — the solitons with the effective diffraction eliminated. The latter, due to their small spatial size, might be of interest for parallel information processing. We prove that the reported effect of size reduction lies solely on the modification of effective diffraction of the system, as the reduced Eq. (9) perfectly reproduces the effect. Also, we show indirectly, that the dominating diffraction is of third order for the midband soliton, as the soliton attains a shape typical for that in material with dominating third order dispersion.

## ACKNOWLEDGMENTS

The work has been partially supported by SFB 407 of DFG, and NATO Collaborative Linkage Grant No. 979050. Discussions with C. O. Weiss, R. Vilaseca, C. Serrat, and R. Herrero are gratefully acknowledged.

## APPENDIX

We derive here the order parameter equation from the equation system (7), by adiabatic elimination of the sideband field components. We assume that the nonlinear part of (7b), i.e., the projection of the nonlinearity $N_{1,2}(A_0, A_{1,2})$, into the sideband spatial wave components is of the higher order of smallness, than the rest of the r.h.s. terms of (7b). This assumption is legitimate for most of the nonlinear systems derived by using multiscale expansion [17], where one generally assumes two temporal scales: one temporal scale $t_1 = O(\varepsilon)$ associated with the linear effects (diffraction, resonator detuning), and the other, slower temporal scale $t_2 = O(\varepsilon^2)$ associated with the build-up and saturation (i.e., nonlinearity) of the radiation in the resonator. Having this in mind one can straightforwardly eliminate the sideband field components $A_{1,2}$ from (7b):

$$A_{1,2} = \frac{-im}{id(\nabla + ik_{1,2})^2} A_0. \tag{A1}$$

The expression (A1) means that the sideband field components are fields that are enslaved by the homogeneous field component solely due to the scattering on the refraction index grating, and not due to nonlinearity.

Further simplification of (A1) is possible by employing the smallness condition $|\nabla| \ll |k_{1,2}|$, which means that the

spatial scales are well separated, and expanding (A1) in power series:

$$A_{1,2} = \frac{m}{dk_{1,2}^2}\left(1 + \frac{2i\nabla}{k_{1,2}} - \frac{3\nabla^2}{k_{1,2}^2} + \cdots\right)A_0. \quad \text{(A2)}$$

Inserting (A2) into (7a) one obtains:

$$\frac{\partial A_0}{\partial t} = N_0(A_0) + id_{\text{eff}}\nabla^2 A_0 - v_{\text{gr}}\nabla A_0 - i\omega_{\text{eff}}A_0. \quad \text{(A3)}$$

With the net diffraction coefficient:

$$d_{\text{eff}} = d\left(1 - \frac{3m^2}{d^2k_1^4} - \frac{3m^2}{d^2k_2^4}\right). \quad \text{(A4a)}$$

The net group velocity of coupled fold components:

$$v_{\text{gr}} = 2dk_0 + 2dk_1\frac{m^2}{d^2k_1^4} + 2dk_2\frac{m^2}{d^2k_2^4}. \quad \text{(A4b)}$$

And the oscillation frequency

$$\omega_{\text{eff}} = -dk_0^2 + \frac{m^2}{dk_1^2} + \frac{m^2}{dk_2^2}. \quad \text{(A4c)}$$

Rewriting (A4a)–(A4c) in terms of modulation depths $f = 2m/(dq^2)$ one obtains

$$d_{\text{eff}} = d\left(1 - \frac{3f^2}{4}\left(\frac{1}{(k-1)^4} + \frac{1}{(k+1)^4}\right)\right), \quad \text{(A5a)}$$

$$v_{\text{gr}} = 2dq\left(k + \frac{f^2}{4}\left(\frac{1}{(k-1)^3} + \frac{1}{(k+1)^3}\right)\right), \quad \text{(A5b)}$$

$$\omega_{\text{eff}} = -dq^2\left(k^2 - \frac{f^2}{4}\left(\frac{1}{(k-1)^2} + \frac{1}{(k+1)^2}\right)\right), \quad \text{(A5c)}$$

which is compatible with the coefficients in (4a), (4b), and (5) in corresponding limits.


[1] D. W. McLaughlin, J. V. Moloney, and A. C. Newell, Phys. Rev. Lett. **51**, 75 (1983); N. N. Rosanov and G. V. Khodova, Opt. Spectrosc. **65**, 449 (1988); M. Tlidi, P. Mandel, and R. Lefever, Phys. Rev. Lett. **73**, 640 (1994).

[2] N. N. Rosanov, J. Opt. Soc. Am. B **7**, 1057 (1990), S. V. Fedorov, A. G. Vladimirov, G V. Khodova, and N. N. Rosanov, Phys. Rev. E **61**, 5814 (2000).

[3] R. Vilaseca, M. C. Torrent, J. García-Ojalvo, M. Brambilla, and M. San Miguel, Phys. Rev. Lett. **87**, 083902 (2001).

[4] K. Staliunas and V. J. Sanchez-Morcillo, Opt. Commun. **139**, 306 (1997); C. Etrich, U. Pechel, and F. Lederer, Phys. Rev. Lett. **79**, 2454 (1997); K. Staliunas and V. J. Sanchez-Morcillo, Phys. Rev. A **57**, 1454 (1998); M. Tlidi, P. Mandel, and M. Haelterman, Phys. Rev. E **56**, 6524 (1997); M. Tlidi and P. Mandel, Phys. Rev. A **56**, R2575 (1999).

[5] D. Michaelis, U. Peschel, and F. Lederer, Phys. Rev. A **56**, R3366 (1997); M. Brambilla, L. A. Lugiato, F. Prati, L. Spinelli, and W. J. Firth, Phys. Rev. Lett. **79**, 2042 (1997).

[6] V. B. Taranenko, K. Staliunas, and C. O. Weiss, Phys. Rev. A **56**, 1582 (1997); G. Slekys, K. Staliunas, and C. O. Weiss, Opt. Commun. **149**, 113 (1998).

[7] V. B. Taranenko, K. Staliunas, and C. O. Weiss, Phys. Rev. Lett. **81**, 2236 (1998).

[8] V. B. Taranenko, I. Ganne, R. J. Kuszelewicz, and C. O. Weiss, Phys. Rev. A **61**, 063818 (2000); S. Barland, Nature (London) **419**, 699 (2002).

[9] G. S. McDonald and W. J. Firth, J. Opt. Soc. Am. B **7**, 1328 (1990); W. J. Firth and A. J. Scroggie, Phys. Rev. Lett. **76**, 1623 (1996).

[10] D. N. Cristodoulides and R. I. Joseph, Opt. Lett. **13**, 794 (1988); A. Aceves, C. De. Angeles, T. Pechel, R. Muschall, F. Lederer, S. Trillo, and S. Wabnitz, Phys. Rev. E **53**, 1172 (1996).

[11] A. C. Scott and L. Macneil, Phys. Lett. **98A**, 87 (1983); S. Darmanyan, A. Kobyakov, F. Lederer, and L. Vazquez, Phys. Rev. B **59**, 5994 (1998).

[12] A. Kobyakov, S. Darmanyan, T. Pertsch, and F. Lederer, Phys. Rev. E **57**, 2344 (1998); T. Pechel, U. Peschel, and F. Lederer, *ibid.* **57**, 1127 (1998).

[13] See, e.g., F. Lederer, S. Darmanyan, and A. Kobyakov, in *Spatial Solitons*, edited by S. Trillo and W. Torruellas (Springer, Heidelberg, 2001).

[14] K. Staliunas, Phys. Rev. Lett. **91**, 053901 (2003).

[15] M. Miyagi and S. Nishida, Appl. Opt. **18**, 678 (1979).

[16] H. S. Eisenberg, Y. Silberberg, R. Marandotti, and J. S. Aitchison, Phys. Rev. Lett. **85**, 1863 (2000).

[17] K. Staliunas, Phys. Rev. A **48**, 1573 (1993); J. Lega, J. V. Moloney, and A. C. Newell, Phys. Rev. Lett. **73**, 2978 (1994).